AGQSM (Augmented Generalized Quadrature Spatial Modulation): Performance evaluation in spatially correlated channels for next-generation wireless communications

Sagar Patel¹, Dharmendra Chauhan¹ Hardik Modi¹, Sagar Kavaiya², and Yogesh Trivedi³

- ¹ EC Department, C S Patel Institute of Technology- CHARUSAT, Changa, Gujarat, India sagarpatel.phd@gmail.com,
- ² C M Patel Institute of Computer Application- CHARUSAT, Changa, Gujarat, India
- ³ EC Department, Institute of Technology, Nirma University, Ahmedabad, Gujarat, India

Abstract. The global impact of 4G brought about increases in mobile usage and network performance. 5G is building on this momentum, bringing substantial network improvements, including higher connection speeds, mobility, and capacity, as well as low-latency capabilities. In the recent technological development, 5G technology is on fore front for development of wireless connectivity between any two points on the earth compared to other technologies such as satellite, optical, WiMAX, WiFi or Bluetooth. It uses multiple antenna deployed at transmitter and receiver side which are actually spatially correlated to each other as less spacing between adjacent antennas and non-uniform scattering in wireless propagation. It degrades the error rate performance. Moreover, the demand for higher spectral efficiency is ever increasing. The Generalized Quadrature Spatial Modulation (GQSM) has recently been proposed to improve the spectral efficiency. This research work examines the transmit antenna correlation effect's in terms of bit error rate (BER) analysis for GQSM - Quasi orthogonal space time block codes (QOSTBC). We use three distinct detection strategies for QOSTBC while analysing a BER performance of three detection schemes for the GQSM. For the investigation, different transmit antenna spacing values of $d_t = 0.1$, 0.2, and 0.4 have been taken into consideration. The experimental results show that at the lower signal to noise ratio(SNR) i.e. SNR=10dB the effect of antenna correlation is low whereas at the higher SNR it is rising. Also, the effect of antenna correlation on one to another become approximately constant for SNR= 20 to SNR= 30. This practical outcome will be helpful in the estimation of the performance analysis....

Keywords: Spatial Modulation, Generalised Quadrature Spatial Modulation, Quasi Orthogonal Space Time Block Code, Spatially correlated Channel, QR decomposition with interference cancellation, Low Complexity Maximum Likelihood (LCML)

1 Introduction

Unprecedented levels of energy and spectrum efficiency are anticipated from fifth generation (5G) wireless networks in order to enable ubiquitous communications between

two devices.[1] [2]. The primary factors directing research towards future wireless communication systems are higher spectral efficiency and data rates. A significant development recently presented for wireless transmission technology in the MIMO communication system is spatial modulation (SM) [1] [2] [3]. Due to the utilization of just a single antenna for transmission, spatial modulation offers the benefit of eradicating inter-channel interference (ICI) and avoiding the need for antenna synchronization, all while still achieving spatial multiplexing gains [1] [2]. Spatial modulation has received a lot of attention in the scientific community as a result of its potential to provide a MIMO implementation that is both spectrally efficient and minimal in complexity [4]. To achieve twice the index bits as SM, quadrature SM (QSM) was proposed in [5-7] to expand index bits to the in-phase/quadrature domain. Furthermore, the space-time domain has been included to the SM/SSK scheme in order to increase the BER efficiency. Examples of this include the differential SM (DSM) in [10, 11], the space-time block coded SM (STBC-SM) in [8, 9], and STSK in [7]. In order to maximize the SE of the conventional QSM scheme, a new SM scheme known as generalised QSM (GQSM) was developed. Three distinct detection algorithms with the lowest possible computational complexity were implemented for GQSM-QOSTBC[12] transmission, presuming uncorrelated channels in the transmit and receive antennas. Despite the fact that practical communication scenarios cannot take spatially uncorrelated pathways into account, this work examines a real-time scenario in which the MIMO system's two ends have spatially correlated channels [13–17]. Under the assumption of antenna correlation at the transmitter and receiver ends of the connection, we provide the BER (bit error rate) performance of the GQSM-QOSTBC.

The rest of this article is structured the following way. The system model and the generation of spatially correlated channels are presented in Section II, different detection methods are described in Section III. Results and discussions are explained in Section IV. Section V deals with conclusions.

2 System Model

In a situation that is somewhat static spatially correlated Rayleigh fading channel scenario, we are examining a MISO system comprising N_t transmitting antennas and a single receiving antenna. Our approach involves implementing a novel transmitter scheme that combines GQSM (Generalized Quadrature Spatial Modulation) with QOSTBC (Quasi-Orthogonal Space-Time Block Coding). Within this system, a variable number, denoted as p, of transmitting antennas from the total N_t antennas is activated for operation. To facilitate the transmission of the real component (I^I) of the modulated signal vector through activated antennas, we employ antenna activation permutation (AAP). Likewise, when it comes to transmitting the imaginary component (I^Q) of the modulated signal vector, a separate AAP is employed for the activated antennas. $C(N_t, p)$ is the total AAPs for both the real and imaginary parts. The modulated signal vector's AAPs are $L = 2^{\lfloor log_2 C(N_t, p) \rfloor}$. In this context, $C(N_t, p)$ represents the choice of picking p antennas from a pool of N_t antennas. Following this, we elucidate the process of GQSM transmission and detection.

The data has splitted into m_1 , m_2 , and m_3 , the total number of input bits (m) was divided. The m_1 characterizes the binary components responsible for M-ary modulation, yielding the modulated signal vector **s** comprising elements $s_1, s_2, ..., s_p$. An initial

vector **s** is formed by $\mathbf{m}1 = p \cdot \log 2(\mathbf{M})$ bits. Here, each element s_{τ} in the vector is expressed as $s_{\tau} = s_{\tau}^{I} + j s_{\tau}^{Q}$ for $1 \leq \tau \leq p$, with s_{τ} belonging to the set χ , which consists of M - ary constellation points. It's worth emphasizing that s_{τ}^{I} and s_{τ}^{Q} are extracted from χ^{I} and χ^{Q} , corresponding to the real and imaginary components of χ , respectively. The real and imaginary parts' index bits are denoted by the bits \mathbf{m}_{2} and \mathbf{m}_{3} , respectively. To compute the AAPs of I^{I} and $\mathbf{m}_{3} = \lfloor log_{2}C(N_{t},p) \rfloor$, bits of $\mathbf{m}_{2} = \lfloor log_{2}C(N_{t},p) \rfloor$ are utilized. The real and imaginary parts of the signals $\{s_{\tau}^{I}\}_{\tau=1}^{p}$ and $\{s_{\tau}^{Q}\}_{\tau=1}^{p}$ are sent using bits for the AAPs of I^{Q} .

Consider \mathbf{s}^I as the real components of the modulated signal vector \mathbf{s} , represented as $[s_1^I, s_2^I, ..., s_p^I]$, and \mathbf{s}^Q as the imaginary components of the modulated signal vector \mathbf{s} , expressed as $[s_1^Q, s_2^Q, ..., s_p^Q]$. Assume that I_{β}^I and I_{α}^I are the β^{th} legal AAPs for I^Q and I^I , respectively, and that they can be expressed as

$$I_{\alpha}^{I} = \{i_{\alpha}^{I}(1), i_{\alpha}^{I}(2), ..., i_{\alpha}^{I}(p)\},\tag{1}$$

as well

$$I_{\beta}^{Q} = \{i_{\beta}^{Q}(1), i_{\beta}^{Q}(2), ..., i_{\beta}^{Q}(p)\},$$
 (2)

correspondingly, $i_{\alpha}^{I}(\eta)$ and $i_{\beta}^{Q}(\eta)$ belong to the set of integers ranging from 1 to N_{t} for values of η between 1 and p. Following this, the real and imaginary sections' $N_{t} \times 1$ signal vectors are as follows:

$$\mathbf{x}^{I} = \{s_{1}^{I}, 0, s_{2}^{I}, \dots 0, s_{p}^{I}\},\tag{3}$$

and

$$\mathbf{x}^{Q} = \{0, s_{1}^{Q}, s_{2}^{Q}, 0, \dots 0, s_{p}^{Q}\}, \tag{4}$$

correspondingly, Note that in x^I and x^Q , the non-zero elements are determined by AAPs I^I and I^Q . The final creation of the signal vector, which has dimensions of $N_t \times 1$, is accomplished through the transmission,

$$x = x^I + jx^Q \tag{5}$$

As per [19], the symbol x in (5) is the GQSM Symbol which includes real, imaginary, and zero values for antenna indices.

x is the transmit GQSM symbol of $N_t \times 1$; it also contains a zero mean and a covariance matrix. $R_x = Exx^H$] = $\sigma_x^2 I$.

The intricate Gaussian noise vector, denoted as **n**, has an average of zero and a covariance matrix represented by $\mathbf{R}_n = E[\mathbf{n}\mathbf{n}^H] = \sigma_n^2 \mathbf{I}$.

Matrix $\mathbf{h} = [h_1, h_2, h_3, h_4]^T$, where h_i , for $i = 1, \dots, 4$, represents the partially static spatially correlated(associated) Rayleigh fading channel coefficient of the i^{th} transmitting antenna to the receiving antenna. The matrix \mathbf{H} denotes the corresponding channel matrix.

The signal vector that was received given by [18].

$$\begin{bmatrix} y_1 \\ y_2^* \\ y_3 \\ y_4^* \end{bmatrix} = \begin{bmatrix} h_1 & h_2 & h_3 & h_4 \\ h_2^* - h_1^* & h_4^* - h_3^* \\ h_3 & h_4 & h_1 & h_2 \\ h_4^* - h_3^* & h_2^* - h_1^* \end{bmatrix} \begin{bmatrix} x_1 \\ x_2 \\ x_3 \\ x_4 \end{bmatrix} + \begin{bmatrix} n_1 \\ n_2^* \\ n_3 \\ n_4^* \end{bmatrix}$$
(6)

Algorithm 1 Transmit Receive antennas correlation Algorithm

In a single column vec(H), layer all H elements

$$vec(H) = egin{bmatrix} h_{1,1} \\ h_{2,1} \\ h_{3,1} \\ h_{4,1} \end{bmatrix}$$

The matrices representing the transmitter ρ_t along with the receiver ρ_r could be represented in the subsequent manner,

$$\rho_{\mathbf{t}} = \begin{bmatrix} E[h_{1,1}h_{1,1}^*] & E[h_{1,1}h_{2,1}^*] & E[h_{1,1}h_{3,1}^*] & E[h_{1,1}h_{4,1}^*] \\ E[h_{2,1}h_{1,1}^*] & E[h_{2,1}h_{2,1}^*] & E[h_{2,1}h_{3,1}^*] & E[h_{2,1}h_{4,1}^*] \\ E[h_{3,1}h_{1,1}^*] & E[h_{3,1}h_{2,1}^*] & E[h_{3,1}h_{3,1}^*] & E[h_{3,1}h_{4,1}^*] \\ E[h_{4,1}h_{1,1}^*] & E[h_{4,1}h_{2,1}^*] & E[h_{4,1}h_{3,1}^*] & E[h_{4,1}h_{4,1}^*] \end{bmatrix} \\ \rho_{\mathbf{r}} = \begin{bmatrix} E[h_{1,1}h_{1,1}^*] \end{bmatrix}$$

The channel correlation R matrix can be shown as follows $\mathbf{R} = \rho_{\mathbf{t}} \otimes \rho_{\mathbf{r}}$

where "

" is used to represent the Kronecker product.

 $\mathbf{R} = \mathbf{V}\mathbf{D}\mathbf{V}^*$

Vector r 16 \times 1 formation in which every element in r is independently separated and distributed as a complex Gaussian element with a variance of one and a mean of zero.

We may now state the following about vec(H)

$$\operatorname{vec}(\mathbf{H}) = \mathbf{V}\mathbf{D}^{1/2}\mathbf{r}$$

which, in equivalent form, is

$$\mathbf{y} = \mathbf{H}\mathbf{x} + \mathbf{n} = \mathbf{H}(\mathbf{x}^I + j\mathbf{x}^Q) + \mathbf{n},\tag{7}$$

Where, **H** is to be constructed as per the steps of algorithm 4.

The optimal maximum likelihood(ML) detection can be expressed as

$$\hat{\mathbf{x}} = \arg\min_{\mathbf{x}} \|\mathbf{y} - \mathbf{H}\mathbf{x}\|^2 \tag{8}$$

$$\hat{\mathbf{x}} = \arg\min_{\mathbf{x}} \|\mathbf{y} - \mathbf{H}(\mathbf{x}^I + j\mathbf{x}^Q)\|^2$$
(9)

To ensure completeness, we present the three QOSTBC detection techniques employed in [18] in the next section.

3 Detection Methods

We offer three QOSTBC detection strategies in this section [18].

Detection Scheme I Equation (6) can be used to express the received vector as

$$y = Hx + n, (10)$$

where, $x = x^I + ix^Q$.

It is possible to factorize the equivalent channel matrix as,

$$\boldsymbol{H} = \boldsymbol{Q}_1 \boldsymbol{R}_1 = \boldsymbol{Q}_1 \begin{bmatrix} a & 0 & b & 0 \\ 0 & a & 0 & b \\ 0 & 0 & c & 0 \\ 0 & 0 & 0 & c \end{bmatrix}$$
(11)

The unitary matrix is denoted by Q_1 , and the upper triangular matrix is represented by R_1 . On both sides of (10), multiply Q_1^H leftward. The matrix that results is,

$$\begin{bmatrix} \tilde{y}_1 \\ \tilde{y}_2 \\ \tilde{y}_3 \\ \tilde{y}_4 \end{bmatrix} = \begin{bmatrix} a & 0 & b & 0 \\ 0 & a & 0 & b \\ 0 & 0 & c & 0 \\ 0 & 0 & 0 & c \end{bmatrix} \begin{bmatrix} x_1 \\ x_2 \\ x_3 \\ x_4 \end{bmatrix} + \begin{bmatrix} \tilde{n}_1 \\ \tilde{n}_2 \\ \tilde{n}_3 \\ \tilde{n}_4 \end{bmatrix}$$
(12)

Using (11), the Hx can be expressed as

$$\begin{bmatrix} h_4 & h_3 & h_2 & h_1 \\ -h_3^* & h_4^* & -h_1^* & h_2^* \\ h_2 & h_1 & h_4 & h_3 \\ -h_1^* & h_2^* & -h_3^* & h_4^* \end{bmatrix} \begin{bmatrix} x_4 \\ x_3 \\ x_2 \\ x_1 \end{bmatrix}$$
(13)

Consequently, we obtain

$$y = Hx + n = H'x' + n \tag{14}$$

The H' QR decomposition may be found using,

$$\mathbf{H}' = \mathbf{Q}_2 \mathbf{R}_2 = \mathbf{Q}_2 \begin{bmatrix} m & 0 & n & 0 \\ 0 & m & 0 & n \\ 0 & 0 & k & 0 \\ 0 & 0 & 0 & k \end{bmatrix}$$
 (15)

Multiplying the left and right sides of (14) by Q_2^H yields

$$\begin{bmatrix} \tilde{y}'_1 \\ \tilde{y}'_2 \\ \tilde{y}'_3 \\ \tilde{y}'_4 \end{bmatrix} = \begin{bmatrix} m & 0 & n & 0 \\ 0 & m & 0 & n \\ 0 & 0 & k & 0 \\ 0 & 0 & 0 & k \end{bmatrix} \begin{bmatrix} x_4 \\ x_3 \\ x_2 \\ x_1 \end{bmatrix} + \begin{bmatrix} \tilde{n}'_1 \\ \tilde{n}'_2 \\ \tilde{n}'_3 \\ \tilde{n}'_4 \end{bmatrix}, \tag{16}$$

which is able to be stated as

$$\tilde{\mathbf{y}}' = \mathbf{R}_2 \mathbf{x}' + \tilde{\mathbf{n}}' \tag{17}$$

Creating a new matrix by combining the 3^{rd} and 4^{th} row of the (12) with the 3^{rd} and 4^{th} of (16) yields

$$\begin{bmatrix} \tilde{y}_{4}' \\ \tilde{y}_{3}' \\ \tilde{y}_{3} \\ \tilde{y}_{4} \end{bmatrix} = \begin{bmatrix} k & 0 & 0 & 0 \\ 0 & k & 0 & 0 \\ 0 & 0 & c & 0 \\ 0 & 0 & 0 & c \end{bmatrix} \begin{bmatrix} x_{1} \\ x_{2} \\ x_{3} \\ x_{4} \end{bmatrix} + \begin{bmatrix} \tilde{n}_{1}' \\ \tilde{n}_{2}' \\ \tilde{n}_{3} \\ \tilde{n}_{4} \end{bmatrix}$$
(18)

The four symbols have been separated as it is illustrated in (19) and (20). Hence, x_1, x_2, x_3 and x_4 , can be detected in parallel as,

$$\hat{x_1} = \arg\min_{x_1 \in \xi} \|\tilde{y_4}' - kx_1\|^2 \qquad \hat{x_2} = \arg\min_{x_2 \in \xi} \|\tilde{y_3}' - kx_2\|^2$$
(19)

$$\hat{x_3} = \arg\min_{x_3 \in \mathcal{E}} \|\tilde{y_3} - cx_3\|^2 \qquad \hat{x_4} = \arg\min_{x_4 \in \mathcal{E}} \|\tilde{y_4} - cx_4\|^2$$
(20)

The $\hat{x_1}$, $\hat{x_2}$, $\hat{x_3}$ and $\hat{x_4}$ are used to detect GQSM symbol.

Detection Scheme II As per (12), the equation is given as

$$\tilde{\mathbf{y}} = \mathbf{R}_1 \mathbf{x} + \tilde{\mathbf{n}} \tag{21}$$

Subsequently, the LC-ML decoder [18] chooses a maximum likelihood (ML) solution. The vector \hat{x} is composed of four elements: \hat{x}_1 , \hat{x}_2 , \hat{x}_3 , and \hat{x}_4 . The value of ξ from the sample space fulfills the following condition:

$$\hat{x} = \arg\min \|\tilde{y} - R_1 x\|^2 = \arg\min_{x \in \xi} \sum_{k=1}^{4} d_k,$$
 (22)

where d_k for k = 1, ..., 4 are given by

$$d_1 = |\tilde{y}_1 - bx_3 - ax_1|^2 \quad d_2 = |\tilde{y}_2 - bx_4 - ax_2|^2$$
 (23)

$$d_3 = |\tilde{y}_3 - cx_3|^2 \quad d_4 = |\tilde{y}_4 - cx_4|^2 \tag{24}$$

Hence, (22) can be expressed as

$$(\hat{x}_1.\hat{x}_3) = \min_{x_1, x_3 \in \xi} (d_1 + d_3)(x_2.x_4) = \min_{x_2, x_4 \in \xi} (d_2 + d_4)$$
 (25)

The $\hat{x_1}$, $\hat{x_2}$, $\hat{x_3}$ and $\hat{x_4}$ are employed to identify the GQSM symbol.

Detection Scheme III As per the (23) and (24), it is possible to decode the output symbol as

$$\hat{x_3} = \arg\min_{x_3 \in \xi} \|\tilde{y_3} - cx_3\|^2 \qquad \hat{x_4} = \arg\min_{x_4 \in \xi} \|\tilde{y_4} - cx_4\|^2$$
 (26)

$$\hat{x_1} = \arg\min_{x_1 \in \xi} \|\tilde{y}_1 - b\hat{x}_3 - ax_1\|^2 \quad \hat{x_2} = \arg\min_{x_2 \in \xi} \|\tilde{y}_2 - b\hat{x}_4 - ax_2\|^2$$
 (27)

Using this method, we first identify the \hat{x}_3 , \hat{x}_4 using (24), rather than joint detection of two pairs of transmitted symbols using (23) in LC-ML decoder. We can then identify x_1 and x_2 by replacing x_3 and x_4 into (27). When we remove the first and second rows from (16), we obtain

$$\begin{bmatrix} \tilde{y}_1' \\ \tilde{y}_2' \end{bmatrix} = \begin{bmatrix} m & 0 & n & 0 \\ 0 & m & 0 & n \end{bmatrix} \begin{bmatrix} x_4 \\ x_3 \\ x_2 \\ x_1 \end{bmatrix} + \begin{bmatrix} \tilde{n}_1' \\ \tilde{n}_2' \end{bmatrix}$$
 (28)

Then, x_3 and x_4 can be detected as

$$\hat{x}_3 = \arg\min_{x_3 \in \xi} \|\tilde{y}_2' - n\hat{x}_1 - mx_3\|^2 \quad \hat{x}_4 = \arg\min_{x_4 \in \xi} \|\tilde{y}_1' - n\hat{x}_2 - mx_4\|^2$$
 (29)

The following procedures can be used to summarize the D-QR-IC:

- First, identify x_3 and x_4 from (24). x_3 and x_4 should be substituted into (23), after which x_1 and x_2 should be found.
- Replace x_1 and x_2 in equation (28) to obtain the final values of x_3 and x_4 .

GQSM symbol detection is done using the $\hat{x_1}$, $\hat{x_2}$, $\hat{x_3}$, and $\hat{x_4}$.

4 Findings and Analysis

This section presents MIMO BER simulation results compared to average SNR performance for the detection scheme-I (GQSM based LCML method), detection scheme-II(GQSM based D-QR method) and detection scheme-III (GQSM based D-QR-IC method) with various values of d_t for the transmit antenna distance, such as 0.1π , 0.2π , and 0.4π and distance of receive antenna 0.1π with $N_t = 4$, $N_r = 1$, p = 2 and m = 8 using 4-QAM modulation in figure 1.

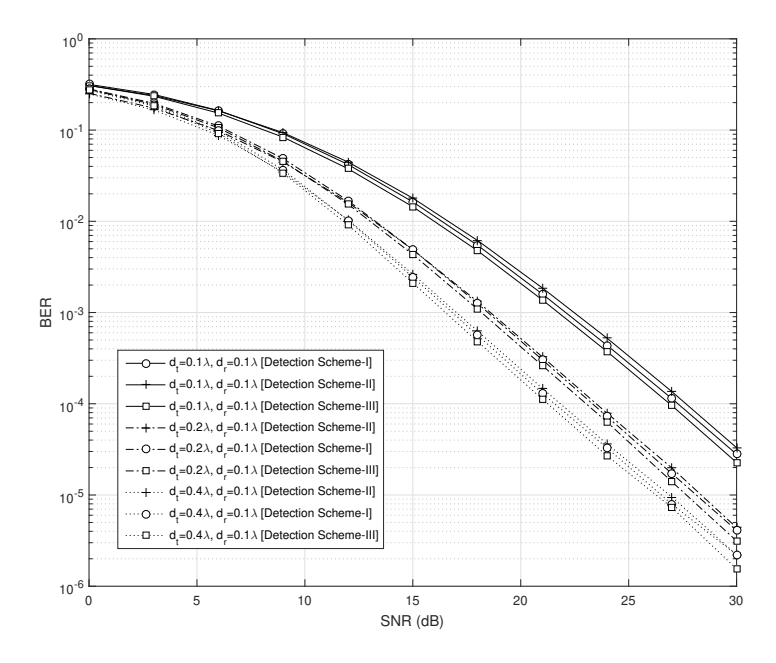


Fig. 1. A comparative analysis of the performance of detection schemes I (LCML), II (DQR), and III (QRIC) is conducted for various values of d_t , including 0.1π , 0.2π , and 0.4π for transmit antenna distance and 0.1π for receive antenna distance, where $N_t = 4$, $N_r = 1$, p = 2, and m = 8 with 4-QAM modulation.

Table 1. Bit error rate provided by $N_t = 4$, $N_r = 1$, p = 2, and m = 8 Generalized Quadrature Spatial Modulation (GQSM) for various detection detection systems using 4-QAM modulation with SNR=10 dB and SNR=30 dB with varied transmit-receive antenna spacing

Conditions	A	В	C	D	E	F
Detection	$d_t = 0.1\pi$	$d_t = 0.1\pi$	$d_t = 0.2\pi$	$d_t = 0.2\pi$	$d_t = 0.4\pi$	$d_t = 0.4\pi$
	$d_r = 0.1\pi$					
Schemes	SNR=10dB	SNR=30dB	SNR=10dB	SNR=30dB	SNR=10dB	SNR=30dB
Detection scheme-I	0.070	0.000038	0.035	0.0000040	0.0120	0.0000030
Detection scheme-II	0.073	0.000024	0.039	0.0000057	0.0140	0.0000021
Detection scheme-III	0.063	0.000029	0.030	0.0000030	0.0150	0.0000016

Figure 1 shows that as the transmission antenna distance is increased, BER performance improves. This demonstrates that a smaller distance between transmit antennas leads to greater antenna correlation. Eventually, it affects the error rate performance of the system. Table 1 demonstrates the bit error rate offered by Generalised Quadrature Spatial Modulation(GQSM) for various detection schemes at the receiver with $N_t = 4$, $N_r = 1$, p = 2, and m = 8 under different antenna separation between the transmitting and receiving ends with SNR=10 dB and SNR=30dB using 4-QAM modulation. Table 1 shows that all three detection schemes have very little variation up to low SNR i.e. 10dB which are shown from condition A, C and E. As the SNR increases from 10dB to 30dB, the BER difference increases from low to high. But the large BER gap between low and high SNR begins at 12dB, justifying the same with all the detection schemes with condition E and F offers approximately 0.01 BER and 0.000003 BER respectively. Also, the BER performance difference between condition **B** and **D** is quite higher than **D** and **E**. This means that shorter distances between transmit antennas have a greater impact on BER performance than longer distances between transmit antennas. Eventually, this turns on to be keep minimum distance between consecutive transmit antennas for desired BER performance. The detection scheme 3 outperform over detection scheme 1 and 2 in all SNR region. Similarly, the detection scheme 2 outperform over detection scheme 1 in all SNR region. These should be quite clear from the BER value of SNR=10dB and SNR=30dB of the different distance illustrated in table 1. The detection complexity of various detection schemes have been demonstrated in table 2. The detection scheme 2 has lowest detection complexity than ML, detection scheme 1 and 3. The computational complexity of detection schemes in terms of number of multiplication/addition have been demonstrated in table 3. Table 2 and 3 shows that detection scheme 2 have least detection complexity and computational complexity than other detection schemes. However, the BER performance of detection scheme 3 offers better results than the other ones in all modulation order due to its additional interference cancellation steps.

 Table 2. The complexity of detection across various detection techniques

Parameter	Detection scheme I		n Detection II scheme I	
Lookup Periods	$2*(S+(S))^2$	† 4*(S)†	6*(S)†	2 ^m

[†] S indicate sample space.

Conclusion

In this article, we have analyzed the BER and computational complexity performance of Generalized Quadrature Spatial Modulation (GQSM) detection techniques with Quasi Orthogonal Space Time Block Code(QOSTBC) under spatially correlated channel. The detection scheme 3 offer better BER performance than other detection scheme 1 and 2. The computational complexity of detection scheme 2 is less compare to other detection scheme 1 and 3. The number of multiplication/addition required for detection schemes under various modulation order have been demonstrated in this article. As the SNR rises from 10dB to 30dB, the BER difference increases from low to high. The lower distance between consecutive transmit antennas play vital role in BER performance than higher distance between consecutive transmit antennas. Hence, the detection schemes offers better error rate performance, less computational complexity and advanced GQSM offers higher spectral efficiency at transmitter. The GQSM - QOSTBC with low computational complexity detection schemes offer spectacular performance in next generation communication systems.

References

- R. Y. Mesleh, H. Haas, S. Sinanovic, C. Ahn and S. Yun: 'Spatial Modulation', *IEEE Trans. on Vehicular Technology*, July 2008, 57(4), p.2228-2247, DOI: 10.1109/TVT.2008.912136
- Y. Bian, X. Cheng, M. Wen, L. Yang, H. V. Poor and B. Jiao: 'Differential Spatial Modulation', *IEEE Transactions on Vehicular Technology*, July 2015, 64(7), p.3262-3268, DOI: 10.1109/TVT.2014.2348791
- 3. R. Patel, S. Patel, and J. Bhalani: 'Performance Analysis and Implementation of different Modulation Techniques in Almouti MIMO Scheme with Rayleigh Channel', *International Conference on Recent Trends in Computing and Communication Engineering*, April 2013, 55(04), p.84-87, DOI:10.3850/978-981-07-6184-4-19
- 4. M. Wen et al., "A Survey on Spatial Modulation in Emerging Wireless Systems: Research Progresses and Applications," in IEEE Journal on Selected Areas in Communications, vol. 37, no. 9, pp. 1949-1972, Sept. 2019, DOI: 10.1109/JSAC.2019.2929453.
- R. Mesleh, S. S. Ikki and H. M. Aggoune, "Quadrature Spatial Modulation," in IEEE Transactions on Vehicular Technology, vol. 64, no. 6, pp. 2738-2742, June 2015, doi: 10.1109/TVT.2014.2344036.
- R. Mesleh, S. Althunibat and A. Younis, "Differential Quadrature Spatial Modulation," in IEEE Transactions on Communications, vol. 65, no. 9, pp. 3810-3817, Sept. 2017, doi: 10.1109/TCOMM.2017.2712720.
- S. Sugiura, S. Chen and L. Hanzo, "Generalized Space-Time Shift Keying Designed for Flexible Diversity-, Multiplexing- and Complexity-Tradeoffs," in IEEE Transactions on Wireless Communications, vol. 10, no. 4, pp. 1144-1153, April 2011, doi: 10.1109/TWC.2011.012411.100065.

- E. Başar, U. Aygölü, E. Panayirci and H. V. Poor, "Space-Time Block Coded Spatial Modulation," in IEEE Transactions on Communications, vol. 59, no. 3, pp. 823-832, March 2011, doi: 10.1109/TCOMM.2011.121410.100149.
- X. Jiang, H. Hai, J. Hou, J. Li and W. Duan, "Euclidean-Geometry-Based Space-Time Block Coded Spatial Modulation," in IEEE Journal of Selected Topics in Signal Processing, vol. 13, no. 6, pp. 1301-1311, Oct. 2019, doi: 10.1109/JSTSP.2019.2922825.
- Y. Bian, X. Cheng, M. Wen, L. Yang, H. V. Poor and B. Jiao, "Differential Spatial Modulation," in IEEE Transactions on Vehicular Technology, vol. 64, no. 7, pp. 3262-3268, July 2015, doi: 10.1109/TVT.2014.2348791.
- 11. J. Li, M. Wen, X. Cheng, Y. Yan, S. Song and M. H. Lee, "Differential Spatial Modulation With Gray Coded Antenna Activation Order," in IEEE Communications Letters, vol. 20, no. 6, pp. 1100-1103, June 2016, doi: 10.1109/LCOMM.2016.2557801.
- 12. Patel, Sagar and Chauhan, Dharmendra and Bhalani, Jaymin and Trivedi, YN, "Novel detection schemes for generalized quadrature spatial modulation," in International Journal of Communication Systems, vol. 34, no. 18, pp. e5001, October 2021, doi: 10.1002/dac.5001.
- S. Mikki, D. Sarkar and Y. Antar: 'Near-field cross-correlation analysis for MIMO wireless communications', *IEEE Antennas Wireless Propag. Lett.*, 2019, 18(7), p.1357, DOI: 10.1109/LAWP.2019.2916627
- D. Tang, X. Xi and J. Zhou: 'A novel MIMO channel model for congested communication environments', *IEEE Access*, 2019,07, p.53754-53765, DOI: 10.1109/AC-CESS.2019.2912321
- S. Kim, H. Cha, J. Kim, S.-W. Ko and S. Kim 'Sense-and-predict: harnessing spatial interference correlation for cognitive radio networks', *IEEE Trans. Wireless Commun.*, May 2019, 18(05), p.2777 2793, DOI: 10.1109/TWC.2019.2908168
- S. Patel, J. Bhalani and Y. Trivedi: 'Performance of Full Rate Non-Orthogonal STBC in Spatially Correlated MIMO Systems', *Radioelectronics and Communications Systems*, 2020, 63(02), p.88-95, DOI: 10.3103/S0735272720020041
- S. Patel, J. Bhalani: 'Near Optimal Receive Antenna Selection Scheme for MIMO System under Spatially Correlated Channel', *International Journal of Electrical and Computer Engi*neering, 2018, 08(05), p.3732-3739, DOI: 10.11591/ijece.v8i5.pp3732-3739
- 18. Gao M, Zhang L, Han C, Ge J.: 'Low-Complexity Detection Schemes for QOSTBC With Four-Transmit-Antenna', *IEEE Communications Letters*, 2015, **19**(15), p.1053-1056, DOI: 10.1109/LCOMM.2015.2417883
- Patel, S., Chauhan, D., Bhalani, J., Trivedi: 'Novel detection schemes for generalized quadrature spatial modulation', *International Journal of Communication Systems*, 2021, 34(18), e5001, DOI: 10.1002/dac.5001